

AIAA 82-4233

# Comparison of Sharp and Blunt Fin-Induced Shock Wave/Turbulent Boundary-Layer Interaction

David S. Dolling\*

*Princeton University, Princeton, New Jersey*

In this paper, results are presented from an experimental study of fin-induced shock wave/turbulent boundary-layer interaction. Semi-infinite fin models, with sharp and hemicylindrically blunted leading edges, were tested at Mach 3 in two high Reynolds number, adiabatic wall, turbulent boundary layers. Detailed streamwise surface pressure distributions were measured at several spanwise stations for angles of attack from 0 to 12 deg. The objective was to examine the spanwise development of the interaction region and determine its dependence on leading edge geometry and the incoming-flow parameters. The results show that for blunt fins there is a region of the interaction in the vicinity of the centerline where the scale and characteristics of the disturbed flowfield are controlled primarily by the leading edge diameter. Outboard of this inner, or "leading-edge dominated," region the interaction properties and spanwise development are essentially the same as if the leading edge were sharp. Thus there is an outer region of the blunt fin-induced flowfield in which the properties are effectively "independent of leading edge blunting."

## Nomenclature

- $D$  = blunt fin leading-edge diameter  
 $h$  = fin height  
 $Lu$  = upstream influence measured relative to the freestream shock wave  
 $M$  = Mach number  
 $P$  = static pressure  
 $P_2$  = wall pressure downstream of interaction  
 $Re$  = Reynolds number  
 $X$  = coordinate in the plane of the test surface and aligned with the tunnel axis, with  $X=0$  at the fin leading edge  
 $X_s$  = coordinate in the  $X$  direction measured relative to the freestream shock wave  
 $Y$  = coordinate normal to the  $X$  axis in the plane of the test surface, with  $Y=0$  at the fin leading edge  
 $Z$  = coordinate normal to the  $XY$  plane measured along the fin leading edge;  $Z=0$  is at the fin root  
 $\alpha$  = fin angle of attack  
 $\beta$  = local angle of blunt fin shock wave  
 $\beta_s$  = sharp fin shock wave angle (Fig. 4)  
 $\delta$  = boundary-layer thickness

## Subscripts

- $\infty$  = undisturbed freestream value  
 $w$  = value at the wall

## Introduction

THE interaction of a shock wave with a turbulent boundary layer is a complex fluid mechanical problem that has been studied by many investigators over a wide range of conditions. Today it is an area still receiving considerable attention. Much of the motivation for such sustained interest in these interactive flowfields stems from their practical importance. They can occur in many types of engine inlets, in turbomachinery, and in a wide variety of external aerodynamic problems. These range from the classic fin/body junction flowfield to that caused by an externally generated impinging shock wave.

A large proportion of the studies of these phenomena concentrated on two-dimensional (2-D) interactions, such as those generated by an unswept compression corner. The general properties and overall behavior of such flows are now reasonably well understood. Comprehensive reviews of experimental results and theoretical approaches have been compiled by Green<sup>1</sup> and Hankey and Holden.<sup>2</sup> More recently, a review of some of the analytical and numerical methods developed during the last 10 years was given by Adamson and Messiter.<sup>3</sup> These major efforts in the 2-D regime contrast sharply with the small amount of attention given to three-dimensional (3-D) interactions. These occur in the vast majority of practical cases, yet at present are not well understood.

To date, the few studies of 3-D interactions have been mainly experimental. It is only during the last few years, with the concurrent development of numerical methods and high-speed computers with large core storage capacity, that it has become possible to compute certain types of these flowfields.<sup>4,5</sup> In many experiments, the shock wave was generated using fin models<sup>6-24</sup> or circular cylinders<sup>24-29</sup> mounted normal to a flat surface on which the incoming boundary layer develops. Fins with sharp<sup>6-14</sup> and blunt<sup>15-24</sup> leading edges have been tested. The blunt fins generally had hemicylindrical leading edges, characterized by diameter  $D$ , although other types, such as flat-faced models, have also been used.<sup>26,30</sup>

Most of the experimental data consist of surface measurements, mainly pressure distributions and oil streak patterns, although some heat-transfer-rate measurements<sup>7,10,25</sup> have been made. Only a few experimenters, notably Oskam<sup>7</sup> and Peake,<sup>9</sup> obtained the detailed flowfield measurements needed for defining interaction structure and for properly validating numerical code predictions. Both examined the sharp fin-induced flowfield. As far as is known, no similar measurements have been made using blunt fins, and although some details of the mean centerline structure are known,<sup>19</sup> the major portion of the flowfield structure has not been determined experimentally.

From these surface measurements, such primary interaction properties as upstream influence have been obtained.<sup>6,15,26,27</sup> A common problem in all 3-D test programs is that defining the interaction properties adequately requires measurements over a large test area at each flow condition. Extensive instrumentation is needed and many tests must be made,

Received Dec. 11, 1981; revision received March 17, 1982. Copyright © American Institute of Aeronautics and Astronautics, Inc., 1982. All rights reserved.

\*Research Staff Member and Lecturer, Dept. of Mechanical and Aerospace Engineering, Member AIAA.

making even the most limited parametric studies expensive and time-consuming. Consequently, such fundamental properties as the streamwise scale, spanwise development, and their dependence on fin geometry and flow conditions are unknown for many of these 3-D interactions.

In studies using hemicylindrically blunted fins or circular cylinders, most investigators concentrated on the centerline and its vicinity. With fins, the majority of tests were made at zero angle of attack. Correlations of the results<sup>15,24,26,27</sup> have shown that the centerline interaction properties depend primarily on  $D$  and only weakly on boundary-layer thickness  $\delta$ . Centerline upstream influence relative to the fin leading edge fell in the narrow band of  $2-3D$  for tests using many different fins over a wide range of flow conditions. Recently it has been shown that upstream influence depends critically on the state of the incoming layer.<sup>25</sup> With a laminar layer at Mach 5, it was observed to be in the range of  $9-12D$ .

These centerline results raise important practical questions that cannot be answered using available data. The questions concern the spanwise development of the blunt fin flowfield. At stations off centerline, is the flowfield scale primarily dependent on  $D$ , or do other parameters affect it? Assuming that this dependence is valid out to some spanwise station, several more questions then arise: 1) Where is this position? 2) On what does it depend? 3) What are the parameters controlling further spanwise development? A second set of questions, of a more general nature but closely connected to these, concerns the relationship between blunt and sharp fin-induced interactions. It is clear that the two flowfields have radically different properties near the leading edge. This fact raises the question of whether these two interactions have quite different scales and characteristics throughout their respective flowfields, or if there are regions in which the properties are similar. In the experimental program described in this paper, an attempt has been made to answer these fundamental questions.

## Experimental Program

### Wind Tunnel and Models

The tests were all conducted in Princeton University's 20-cm  $\times$  20-cm (8-in.  $\times$  8-in.), high Reynolds number, supersonic blowdown tunnel. This facility has a nominal freestream Mach number of 3 and can be operated at stagnation pressures over the range  $4 \times 10^5$  to  $3.4 \times 10^6$   $\text{Nm}^{-2}$  (60-500 psia).

The model geometry is sketched in Fig. 1. Two test surfaces were used: the tunnel floor, and a horizontal flat plate with a sharp leading edge that spanned the tunnel. Both surfaces were instrumented with four rows of pressure tapings aligned with the undisturbed-flow direction. The tapings were 0.102 cm (0.040 in.) in diameter and had a minimum spacing of 0.25 cm (0.10 in.).

The fin models were all 25 cm (10 in.) long and spanned the tunnel. Nylon seals at the floor and ceiling junctions prevented leakage. They were supported by bearings centered 2.29 cm (0.90 in.) downstream of the leading edge and by an arm attached to the rear face. The arm passed through the tunnel sidewall to a drive mechanism allowing the angle of attack  $\alpha$  to be changed from outside the tunnel. In tests using the tunnel floor boundary layer, the fin leading edge was approximately 20 cm (8 in.) downstream of the nozzle exit plane. For the flat-plate tests, it was about 22 cm (9 in.) downstream of the plate leading edge.

The blunt models tested on the tunnel floor had  $D = 0.318, 0.635, 0.952, \text{ and } 1.27$  cm (0.125, 0.250, 0.375, and 0.5 in.). Those used with the flat plate had  $D = 0.102, 0.203, 0.305, \text{ and } 0.406$  cm (0.040, 0.080, 0.120, and 0.160 in.). Sharp fins were also used with both test surfaces. Based on the criterion described in Ref. 15, the height  $h$  of all the blunt models was large enough for them to be considered semi-infinite. A fin described as semi-infinite is one that produces the "asymptotic result," a condition occurring when further increases in  $h$  do not increase the extent of the disturbed flowfield.

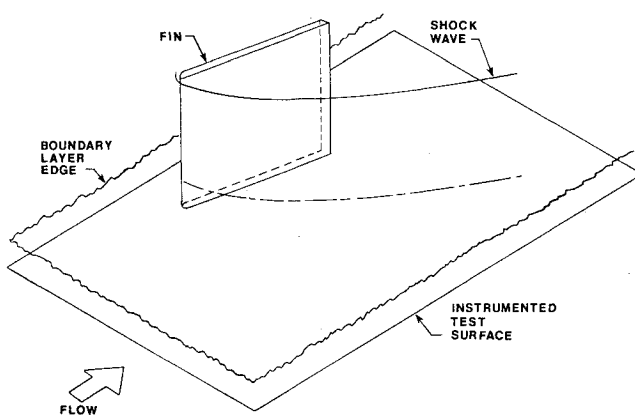


Fig. 1 Model configuration.

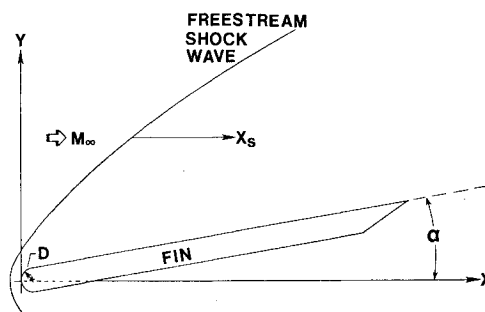


Fig. 2 Coordinate system.

otic result," a condition occurring when further increases in  $h$  do not increase the extent of the disturbed flowfield.

The coordinate system used for presentation of the results is shown in Fig. 2. It is drawn for a blunt leading edge but applies equally to the sharp case. For the latter, the origin of the  $X$ - $Y$  axes is at the sharp edge. In both cases, the streamwise distance  $X_s$  is measured from the freestream shock wave location.

### Test Conditions and Incoming Boundary Layers

All tests were made at a stagnation pressure of  $6.8 \times 10^5$   $\text{Nm}^{-2} \pm 1\%$  (100 psia). The stagnation temperature was  $260 \text{ K} \pm 5\%$ , and the model wall temperature was approximately adiabatic. These flow conditions gave a nominal freestream Reynolds number  $Re_\infty$  of  $6.5 \times 10^7 \text{ m}^{-1} \pm 5\%$ .

No boundary-layer trips were used. On the flat plate, natural transition occurred within 2 cm (0.8 in.) of the leading edge. The streamwise growth of the tunnel floor and flat-plate boundary layers have been measured. The boundary layers are two-dimensional and in equilibrium, and their mean-velocity profiles match the wall-wake similarity law. The thickness of the undisturbed layer at the location of the fin leading edge was 1.25 cm (0.49 in.) on the tunnel floor and 0.25 cm (0.1 in.) on the flat plate. Since these interactions are swept, the local incoming boundary-layer thickness increases in the spanwise direction. Values of  $\delta$  given in the legends of the figures are the local values immediately upstream of the initial pressure rise.

### Shock Wave Shape

Since the position  $X_s = 0$  is a streamwise reference point, it was necessary that the shock wave shapes be known accurately. They were obtained experimentally from full-scale shadow photographs of the flow over a set of sting-mounted wedges spanning the ranges of  $D$  and  $\alpha$  used in the test program. For consistency and accuracy, the shock wave angles for the sharp fin were also obtained experimentally, rather than from oblique shock wave theory. Although viscous effects at the leading edge are typically small, small

errors in angle can result in large errors in locating the position  $X_s=0$ , particularly along instrumentation lines far from the fin.

Discussion of Results

Recent results,<sup>15</sup> in conjunction with those from earlier studies,<sup>21,24</sup> showed that centerline pressure distributions upstream of blunt leading edges could be correlated by normalizing the streamwise distance  $X$  by  $D$ . This simple scaling method worked well for flows in which  $\delta$  varied by about 46:1. Leading edge pressure distributions could also be correlated in a similar way by normalizing the distance from the fin root  $Z$  by  $D$ .<sup>15</sup> This strong dependence on  $D$ , in both the horizontal and vertical planes, is the reason why the critical parameter in determining whether or not a fin (or cylindrical protuberance) can be considered semi-infinite is  $h/D$  and not  $h/\delta$ . This is an important point, since it has often been wrongly assumed that, if  $h/\delta > 1$ , the extent of the disturbed flowfield would have reached a maximum.

This same strong dependence on  $D$  has also been observed off centerline.<sup>16</sup> Streamwise pressure distributions generated by different-diameter fins in different boundary layers could be correlated at a common nondimensional spanwise station  $Y/D$  when plotted as a function of  $X_s/D$ . Good correlations were obtained over a range of fin angles of attack. This inner region of the blunt fin-induced flowfield, in which  $D$  plays a critical role, may aptly be described as being "leading-edge dominated." The spanwise extent of this region and on what it depends are discussed later.

An attempt to correlate all the blunt fin results in this way was unsuccessful. A progressively larger data spread occurred with increasing  $Y/D$ . However, dimensional plots showed that, at a certain spanwise station, pressure distributions generated using different bluntnesses all had essentially the same physical length scale and the same general features. Further, these were the same, within engineering accuracy, as those generated at the same station using a sharp fin. An example is shown in Fig. 3. These five distributions were generated using four blunt fins and a sharp model at  $\alpha=10$  deg. They were measured on the flat-plate model along a fixed row of taps at  $Y \sim 3.4$  cm (1.34 in.). There is a systematic increase in  $Y$  with increasing  $D$  but, as the legend shows, it is small. The variation is about  $\pm 3\%$  of the mean value, and does not affect the comparisons, since for any given interaction such a change has a very small effect on the flowfield properties. At this station, blunting the fin leading edge over the range shown has little effect on the interaction scale and features. For this reason, the station is in the "outer region" of the four blunt fin-induced flowfields. Here the properties are effectively "independent of leading edge blunting." Once in this outer region, the spanwise development of the blunt fin flowfield is the same as that of the sharp model.

Tests using sharp fins<sup>6</sup> have shown that the interaction scale, in both streamwise and spanwise directions, depends on  $\delta$ . It was shown above that at some spanwise station the blunt fin-induced flowfield acquires the same characteristics as the sharp case, and then both develop in the same way. This means that, for blunt fins, the interaction changes from one whose scale is dominated by  $D$  in the inner region to one whose spanwise development in the outer region depends on  $\delta$ .

Whether or not a given station is in the outer region depends on its position in terms of  $Y/D$ . The reason involves the angle-of-attack characteristics of blunt and sharp fin-induced shock wave shapes. With sharp fins the shock waves are attached and straight, and their angle  $\beta_s$  is a function only of  $\alpha$ . In contrast, as shown in Fig. 4, with a blunt leading edge, the shock is detached and curved, and the local angle  $\beta$  depends on position. Further, in the region around the leading edge,  $\beta$  is independent of  $\alpha$ . Measurements taken from the shadow photographs showed that the shock shapes generated by different diameter leading edges could be correlated if

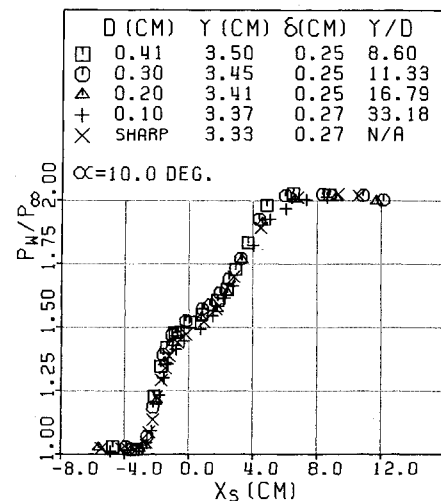


Fig. 3 Outer region pressure distributions.

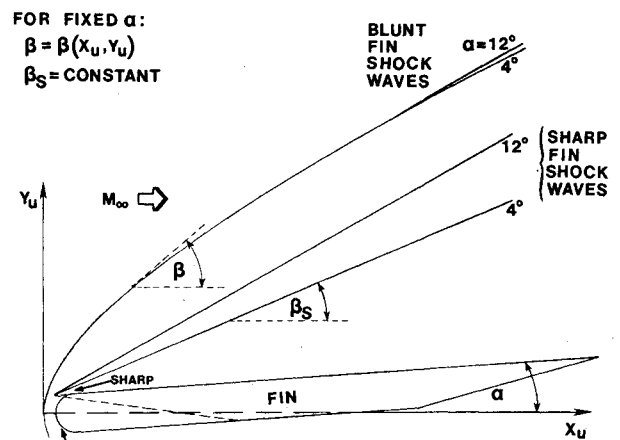


Fig. 4 Effect of blunting on shock wave shape.

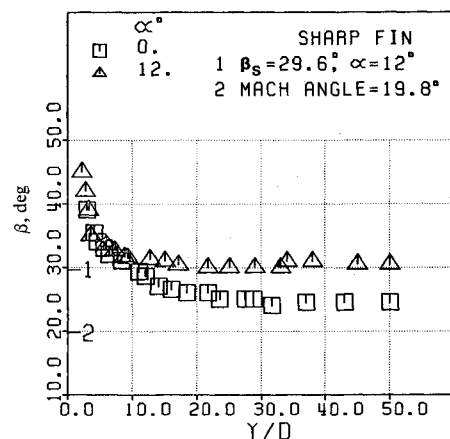


Fig. 5 Blunt fin shock wave angles.

plotted as  $X_u/D$  vs  $Y_u/D$ .  $X_u$  and  $Y_u$  are defined in Fig. 4. This scaling worked well for small  $Y/D$ , but with increasing spanwise distance, each value of  $\alpha$  generated a separate curve.

An alternative method of presenting the same data, shown in Fig. 5, is to plot  $\beta$  vs  $Y/D$ . Two curves are shown: for  $\alpha=0$  and  $12$  deg. With this approach, a direct comparison can be made with the sharp fin shock wave angles. These are also shown in Fig. 5. Close to the leading edge,  $\beta$  and  $\beta_s$  are radically different. As  $Y/D$  increases, however,  $\beta$  rapidly approaches  $\beta_s$ . For  $\alpha=10$  or  $12$  deg,  $\beta$  is only 2-3 deg higher

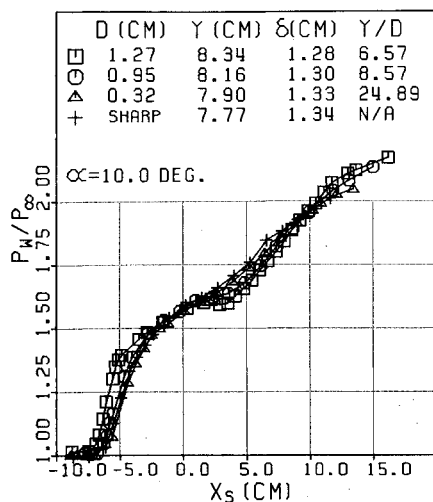


Fig. 6 Shift from outer to inner region with increasing blunting.

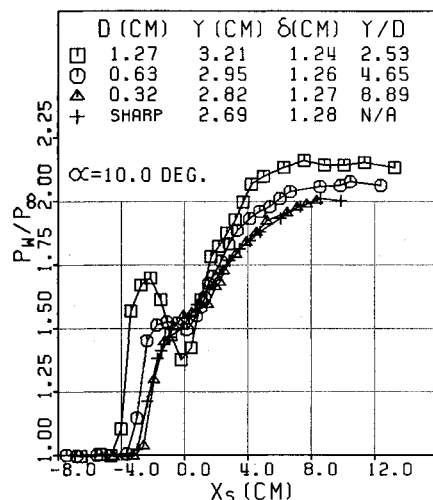


Fig. 7 Further shift from outer to inner region with increasing blunting.

than  $\beta_s$  at  $Y/D$  of about 7-8. The value of  $Y/D$  at which  $\beta$  and  $\beta_s$  differ by some small amount increases as  $\alpha$  decreases. Thus, for blunt fins, there is some spanwise station  $Y/D$  at which the local shock wave angle becomes the same as that which would occur if the leading edge were sharp.

Now, in Fig. 3 it was seen that the spanwise station  $Y \sim 3.4$  cm (1.34 in.) was in the outer region of the four blunt fin flowfields. The values of  $Y/D$  fell in the range 8.6-33.2. The shock-angle plot shows that, for this range at  $\alpha = 10$  deg, all four values of  $\beta$  are very close to one another and close to  $\beta_s$ . Thus at this spanwise station, both the local shock wave angles and the overall interaction pressure rises,  $P_2/P_\infty$  (i.e., fixed  $\alpha$ ) are essentially the same for the blunt and sharp fins. Under these two conditions and with the same incoming boundary layer, sharp and blunt fin-induced interactions have the same local scale and characteristics. At  $\alpha = 10$  deg, the only condition necessary for ensuring that  $\beta$  at some station  $Y$  is close to  $\beta_s$  is simply that  $Y/D > \sim 8$ . This is the case for the data of Fig. 3. Although  $Y/D$  may take any value greater than this minimum, the value of  $Y$  itself must be fixed. The reasons for this are discussed later.

If all other parameters are held fixed, then at any spanwise station an increase in  $D$  simply decreases  $Y/D$ . At  $\alpha = 10$  deg,  $\beta$  will only increase slightly with decreasing  $Y/D$  if  $Y/D > \sim 8$ . If  $Y/D$  falls below  $\sim 8$ ,  $\beta$  increases rapidly, with a corresponding change in the scale and features of the pressure distribution. The increase in  $D$  results in the station's being

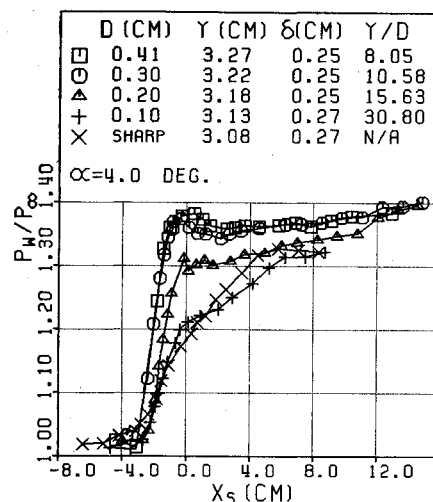


Fig. 8 Shift from outer to inner region with decreasing angle of attack.

shifted inboard into the leading edge-dominated region, as shown in Fig. 6. The four pressure distributions were measured on the tunnel floor at  $Y \sim 8.0$  cm (3.15 in.).  $\alpha = 10$  deg for all cases. The distributions for  $Y/D = 8.57$  and 24.89 do not differ significantly from those generated using a sharp fin and are therefore in the outer region of the flowfield. Decreasing  $Y/D$  from 8.57 to 6.57 causes a change in upstream influence, and the beginning of a change in the shape of the distribution is already noticeable. This trend is even more pronounced in the data shown in Fig. 7. These measurements, made under identical flow conditions, are along the innermost tap row,  $Y \sim 2.9$  cm (1.15 in.). The sharp fin distribution and that corresponding to  $Y/D$  of 8.89 are essentially the same. At  $Y/D = 4.65$  and 2.53,  $P_2/P_\infty$  does not change much, but  $\beta$  has increased significantly, with corresponding changes in the scale and shape of the distribution.

Two comments must be made about these results. First, the boundary between the inner and outer regions which occurs at  $Y/D \sim 8$  will apply only for  $\alpha$  in the neighborhood of 10 or 12 deg. At lower  $\alpha$ ,  $\beta$  and  $\beta_s$  do not come close to one another until larger values of  $Y/D$  are reached. This implies that, for the same range of  $Y/D$  as in Fig. 3, but at lower  $\alpha$ , the pressure distributions would not all correlate. Figure 8 shows that this is the case. The five distributions were generated along the same tap row as in Fig. 3, using the same five leading edges and the same incoming boundary layer, but with  $\alpha$  reduced to 4 deg. Upstream influence does not vary much, but there are major differences in the shapes of the pressure distributions.  $P_2/P_\infty$  does not change significantly for these five flows, but  $\beta$  varies by almost 50%. As would be expected, the distribution closest to that of the sharp fin occurs for the largest value of  $Y/D$ . Thus at  $\alpha = 4$  deg, the boundary between the inner and outer regions has moved out to  $Y/D \sim 30$ .

The results so far show that blunt and sharp fin-induced pressure distributions at a given spanwise station correlate providing all values of  $Y/D$  exceed some minimum value. The second comment is an explanation of why correlations can be obtained only at a fixed  $Y$ , although the values of  $Y/D$  may vary. In Fig. 3, for example,  $Y \sim 8.0$  cm (3.15 in.) whereas  $Y/D$  varies from 6.57 to 24.89. For the largest  $D$  ( $= 1.27$  cm),  $Y/D$  is 6.57, which is below the minimum value of about 8 necessary for the correlation, so for this flow the station is in the inner region. For the other blunt fins,  $Y/D > 8$ , the data sets correlate, and therefore  $Y \sim 8.0$  cm (3.15 in.) is in the outer region. For each flow, however,  $Y \sim 8$  cm (3.15 in.) is a different physical distance away from the boundary that occurs at  $\sim 8D$ . Between  $Y \sim 8D$  and  $Y \sim 8$  cm (3.15 in.), each blunt fin-induced interaction develops spanwise in the same

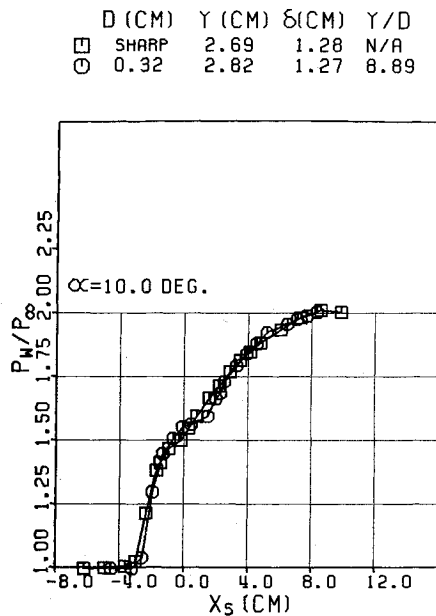


Fig. 9 Common spanwise development of sharp and blunt fin interactions;  $Y \sim 2.75$  cm (1.08 in.).

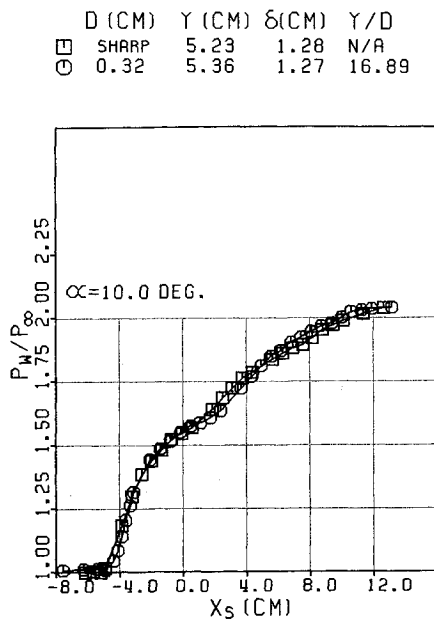


Fig. 10 Common spanwise development of sharp and blunt fin interactions;  $Y \sim 5.3$  cm (2.1 in.).

way as the sharp case. Thus at  $Y \sim 8$  cm the data sets correlate, although  $Y/D$  varies from 8.57 to 24.89. If these same values of  $Y/D$  were generated by fixing  $D$  and varying  $Y$ , the data would obviously not correlate. Each station would correspond to a different position in the sharp fin flowfield and would have a different streamwise scale.

This behavior is illustrated in Figs. 9 and 10, which show sharp and blunt [ $D = 0.317$  cm (0.125 in.)] pressure distributions at  $Y \sim 2.75$  cm (1.08 in.) and  $Y \sim 5.3$  cm (2.1 in.), respectively. These stations are at  $Y/\delta \sim 2.3$  and 4.3. Since  $\alpha = 10$  deg, the boundary of the inner and outer regions of this flowfield will be at  $Y \sim 2.5$  cm (1 in.) (i.e.,  $Y/D \sim 8$ ). The inner row, at  $Y = 2.82$  cm (1.1 in.), is just within the outer region, and the data correlate with those of the sharp fin (Fig. 9). The spanwise development of both flowfields is now the same, as can be seen from the measurements at the next station,  $Y \sim 5.3$

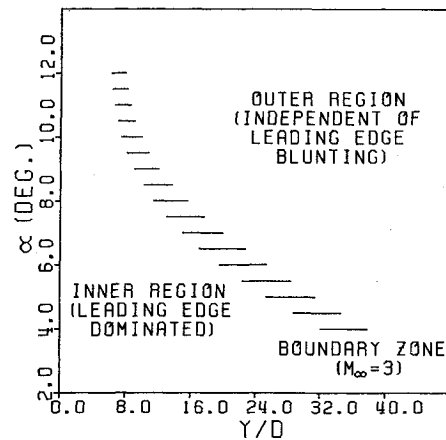


Fig. 11 Boundary zone between inner and outer regions for Mach 3.

cm (2.1 in.) (Fig. 10). Now, if  $D$  were approximately halved, then along the inner row  $Y/D$  would be about 17-18. The new data would still correlate with those already plotted in Fig. 9 since  $Y/D > \sim 8$ . On the other hand, data at the same  $Y/D$  (i.e., 17), such as those in Fig. 10, but generated using the original  $D$ , do not correlate with Fig. 9. The values of  $Y$  are different, each corresponding to a different position in the sharp fin flowfield, and thus each has a different physical scale. The correlation process thus applies for a range of  $Y/D$  at a given  $Y$ , but not for the same range of  $Y/D$  with variable  $Y$ .

Through careful examination of the 280 measured pressure distributions, Fig. 11 was constructed. It defines, as a function of  $\alpha$ , the approximate boundary between the inner and outer regions of the blunt fin-induced interaction. At each station, comparisons were made between the pressure distributions generated by sharp and blunt fins. If the upstream influence, overall length scale, general features, and pressure levels of a given blunt case were essentially the same as those of the sharp case, then that value of  $Y/D$  was considered as being in the outer region. In many cases, such as that of Fig. 10, such a decision is easily made, but in others, mainly at low  $\alpha$ , it is more difficult. An exact boundary cannot be determined, but a zone, the crosshatched area of Fig. 11, can be defined. For  $\alpha < 4$  deg, the data set was insufficient to define even an approximate boundary. At  $\alpha = 0$  deg, the comparison becomes meaningless, since there is no interaction if the leading edge is sharp. The same boundary location was observed for both the tunnel floor and flat-plate tests. It should be noted that Fig. 11 was constructed using data from experiments at a single freestream Mach number. Since the location of the boundary zone is critically dependent on the relationship between blunt and sharp fin shock wave shapes, it could be a function of Mach number.

With this approach, any blunt fin-induced flowfield can be split into two regions. Since the scales and characteristics of the pressure distributions in the inner region differ from those of the sharp case, this area has been labeled "leading-edge dominated." This poses the further question of whether the description implies that 1) anywhere within this region, pressure distributions generated by different-diameter fins in different boundary layers can be correlated at a common value of  $Y/D$  or 2) that point 1 holds over only a certain portion of this inner region. To answer this question fully, tests need to be made at critical regions of the  $\alpha$ - $Y/D$  matrix using many different boundary layers. From the present tests and other investigations, the following can be stated. On centerline (i.e.,  $Y/D = 0$ ), good correlations can be obtained using  $D$  as a distance scaling parameter for flows in which  $0.16$  cm  $\leq D \leq 5.08$  cm ( $0.06$  in.  $\leq D \leq 2$  in.) (i.e., 1:32) and  $0.33$  cm  $\leq \delta \leq 15.24$  cm ( $0.13$  in.  $\leq \delta \leq 6$  in.) (i.e., 1:46). Off centerline, the present tests show that for  $6 \text{ deg} \leq \alpha \leq 12 \text{ deg}$ ,

this correlation technique is applicable over the range of  $Y/D$  defined by Fig. 11. In this case, the range of  $\delta$  used was smaller, about 1:4, and the minimum range of  $D$  for which checkpoints existed was 1:2. Further, other than the centerline results, which spanned the range  $2.9 \leq M_\infty \leq 5$ , the tests were all conducted at a single value of  $M_\infty$ .

These results greatly simplify the general problem of determining the spanwise development of blunt fin-induced interactions. They effectively preclude the need to make measurements over a wide area using many leading edges. The primary task is to determine spanwise development for the sharp fin, since the outer regions of all the blunt cases will be the same. Only a limited series of tests using blunt fins would then be needed 1) to establish the approximate location of the boundary between the inner and outer regions and 2) to confirm that within the inner region  $D$  is the appropriate distance scaling parameter.

### Concluding Remarks

An experimental study was made of fin-induced shock wave/turbulent boundary-layer interaction. The tests were made in a Mach 3, high Reynolds number, blowdown tunnel using fins with sharp and hemicylindrically blunted unswept leading edges. The wall temperature condition was approximately adiabatic. Streamwise surface pressure distributions were measured at several spanwise stations using different fin leading edges and incoming turbulent boundary layers for angles of attack in the range 0-12 deg. The objective of the test program was to investigate spanwise development of the interaction and its dependence on the geometric and flow parameters.

These measurements have shown the following:

1) In the blunt fin-induced interaction, there is an inner region of the flowfield that can be described as leading edge-dominated. Within this region, the scales and characteristics of the interaction differ significantly from those generated using a sharp fin. The properties are dependent primarily on the leading edge diameter  $D$  and are only weakly affected by substantial changes in incoming-boundary-layer thickness  $\delta$ .

2) At a certain spanwise station  $Y$ , the streamwise pressure distribution generated by a blunt fin has the same length scale and general features as one generated at the same  $Y$  but using a sharp fin. Outboard of this spanwise position, the scales and characteristics of both interactions develop in the same way. Thus, for the blunt fin, there is an outer region of the interaction in which the properties are effectively independent of leading edge blunting.

3) Spanwise development of the sharp fin-induced interaction depends on the characteristics of the incoming turbulent boundary layer. This means that, for blunt fins, the interaction changes from one whose properties are controlled by  $D$  in the inner region to one whose development outside the inner region depends mainly on the incoming boundary layer.

4) The approximate location of the boundary zone between the inner and outer regions of the blunt fin-induced flowfield can be specified in terms of a number of leading edge diameters. This number is a function of fin angle of attack. Thus at any station  $Y$ , blunt and sharp fins will have the same scale and characteristics providing all values of  $Y/D$  are greater than the minimum defined by the boundary.

The preceding conclusions are based mainly on tests at a single freestream Mach number. Since they can be related to the angle-of-attack characteristics of blunt and sharp fin-induced shock waves that depend on Mach number, they could be different at other freestream conditions.

### Acknowledgments

This work was supported by the U.S. Air Force Office of Scientific Research under Contract F49620-81-K-0018, monitored by Dr. J. D. Wilson, and by the U.S. Navy, Naval

Air Systems Command, under Contract N60921-81-K-0007, monitored by D. Hutchins. Many useful discussions were held with Dr. G. S. Settles and Professor S. M. Bogdonoff. Their suggestions are gratefully acknowledged.

### References

- <sup>1</sup>Green, J. E., "Interactions Between Shock Waves and Turbulent Boundary Layers," *Progress in Aerospace Sciences*, Vol. 11, 1970, pp. 235-340.
- <sup>2</sup>Hankey, W. L. and Holden, M. S., "Two-Dimensional Shock Wave Boundary Layer Interaction in High Speed Flows," AGARDograph 203, 1975.
- <sup>3</sup>Adamson, T. E. and Messiter, A. F., "Analysis of Two-Dimensional Interactions Between Shock Waves and Boundary Layers," *Annual Review of Fluid Mechanics*, Vol. 12, 1980, pp. 103-138.
- <sup>4</sup>Horstman, C. C. and Hung, C. M., "Computation of Three-Dimensional Turbulent Separated Flows at Supersonic Speeds," AIAA Paper 79-0002, Jan. 1979.
- <sup>5</sup>Hung, C. M. and MacCormack, R. W., "Numerical Solution of Three-Dimensional Shock Wave and Turbulent Boundary Layer," AIAA Paper 78-161, Jan. 1978.
- <sup>6</sup>Dolling, D. S. and Bogdonoff, S. M., "Upstream Influence Scaling of Sharp Fin-Induced Shock Wave Turbulent Boundary Layer Interactions," AIAA Paper 81-0336, Jan. 1981.
- <sup>7</sup>Oskam, B., "Three-Dimensional Flowfields Generated by the Interaction of a Swept Shock Wave with a Turbulent Boundary Layer," Gas Dynamics Lab., Princeton Univ., Princeton, N.J., Rept. 1313; also Ph.D. Thesis, Aerospace and Mechanical Sciences Dept., Princeton Univ., Dec. 1976.
- <sup>8</sup>Oskam, B., Vas, I. E., and Bogdonoff, S. M., "Mach 3 Oblique Shock Wave/Turbulent Boundary Layer Interactions in Three Dimensions," AIAA Paper 76-336, July 1976.
- <sup>9</sup>Peake, D. J., "The Three-Dimensional Interaction of a Swept Shock Wave with a Turbulent Boundary Layer and the Effects of Air Injection on Separation," Ph.D. Thesis, Carleton Univ., Ottawa, Canada, 1975.
- <sup>10</sup>Token, K. H., "Heat Transfer Due to Shock Wave Turbulent Boundary Layer Interactions on High Speed Weapon Systems," AFFDL-TR-74-77, April 1974.
- <sup>11</sup>Law, H. C., "Three-Dimensional Shock Wave Turbulent Boundary Layer Interactions at Mach 6," Aerospace Research Lab., Wright-Patterson Air Force Base, Ohio, ARL-TR-75-0191, June 1975.
- <sup>12</sup>Lowrie, B. W., "Cross-Flows Produced by the Interaction of a Swept Shock Wave with a Turbulent Boundary Layer," Ph.D. Thesis, Cambridge Univ., Cambridge, England, 1965.
- <sup>13</sup>McCabe, A., "A Study of Three-Dimensional Interactions Between Shock Waves and Turbulent Boundary Layers," Ph.D. Thesis, Univ. of Manchester, Manchester, England, 1963.
- <sup>14</sup>Stanbrook, A., "An Experimental Study of the Glancing Interaction Between a Shock Wave and a Turbulent Boundary Layer," Aeronautical Research Council, U.K., ARC-CP-No. 555, 1961.
- <sup>15</sup>Dolling, D. S. and Bogdonoff, S. M., "Scaling of Interactions of Cylinders with Supersonic Turbulent Boundary Layers," *AIAA Journal*, Vol. 19, May 1981, pp. 655-657.
- <sup>16</sup>Dolling, D. S., Cosad, C. D., and Bogdonoff, S. M., "An Examination of Blunt Fin-Induced Shock Wave Turbulent Boundary Layer Interactions," AIAA Paper 79-0068, Jan. 1979.
- <sup>17</sup>Gillerlain, J. D., "Fin-Cone Interference Flow Field," AIAA Paper 79-0200, Jan. 1979.
- <sup>18</sup>Cosad, C. D., "An Analysis of Blunt Fin-Induced Shock Wave-Turbulent Boundary Layer Interactions," M.S.E. Thesis, Aerospace and Mechanical Sciences Dept., Princeton Univ., Princeton, N.J., July 1978.
- <sup>19</sup>Kaufman, L. G., Korkegi, R. H., and Morton, L. C., "Shock Impingement Caused by Boundary Layer Separation Ahead of Blunt Fins," Aerospace Research Lab., Wright-Patterson Air Force Base, Ohio, ARL 72-0118, Aug. 1972.
- <sup>20</sup>Winkelman, A. E., "Experimental Investigations of a Fin Protuberance Partially Immersed in a Turbulent Boundary Layer at Mach 5," Naval Ordnance Laboratory, White Oak, Md., NOL-TR-72-33, Jan. 1972.
- <sup>21</sup>Winkelman, A. E., "Flow Visualization Studies of a Fin Protuberance Partially Immersed in a Turbulent Boundary Layer at Mach 5," Naval Ordnance Laboratory, White Oak, Md., NOL-TR-70-93, May 20, 1970.

<sup>22</sup>Lucas, E. J., "Investigation of Blunt Fin-Induced Flow Separation Region on a Flat Plate at Mach Numbers 2.5 to 4.0," AEDC-TR-70-265, Jan. 1971.

<sup>23</sup>Useton, J. C., "Fin Shock-Boundary Layer Interaction Tests on a Flat Plate with Blunted Fins at  $M=3$  and 5," AEDC-TR-67-113, June 1967.

<sup>24</sup>Price, A. E. and Stallings, R. L., "Investigation of Turbulent Separated Flows in the Vicinity of Fin Type Protuberances at Supersonic Mach Numbers," NASA TN D-3804, Feb. 1967.

<sup>25</sup>Hung, F. T. and Clauss, J. M., "Three-Dimensional Protuberance Interference Heating in High Speed Flow," AIAA Paper 80-0289, Jan. 1980.

<sup>26</sup>Sedney, R. and Kitchens, C. W. Jr., "Separation Ahead of Protuberances in Supersonic Turbulent Boundary Layers," *AIAA Journal*, Vol. 15, April 1977, pp. 546-552.

<sup>27</sup>Westkaemper, J. C., "Turbulent Boundary Layer Separation Ahead of Cylinders," *AIAA Journal*, Vol. 6, July 1968, pp. 1352-1355.

<sup>28</sup>Voitenko, D. M., Zubkov, A. I., and Panov, Y. A., "Supersonic Gas Flow Past a Cylindrical Obstacle on a Plate," *Mekhanika Zhidkosti i Gaza*, Vol. 1, Jan. 1966, pp. 121-125.

<sup>29</sup>Miller, W. H., "Pressure Distributions on Single and Tandem Cylinders Mounted on a Flat Plate in Mach Number 5.0 Flow," Defense Research Lab., Univ. of Texas, Austin, Texas, DRL 538, June 1, 1966.

<sup>30</sup>Dolling, D. S. and Bogdonoff, S. M., "Experimental Investigation of Three-Dimensional Shock Wave Turbulent Boundary Layer Interaction: An Exploratory Study of Blunt Fin-Induced Flows," Dept. of Mechanical and Aerospace Engineering, Princeton, Univ., Princeton, N.J., MAE Rept. 1468, March 1980.

*From the AIAA Progress in Astronautics and Aeronautics Series . . .*

## **AEROTHERMODYNAMICS AND PLANETARY ENTRY—v. 77 HEAT TRANSFER AND THERMAL CONTROL—v. 78**

*Edited by A. L. Crosbie, University of Missouri-Rolla*

The success of a flight into space rests on the success of the vehicle designer in maintaining a proper degree of thermal balance within the vehicle or thermal protection of the outer structure of the vehicle, as it encounters various remote and hostile environments. This thermal requirement applies to Earth-satellites, planetary spacecraft, entry vehicles, rocket nose cones, and in a very spectacular way, to the U.S. Space Shuttle, with its thermal protection system of tens of thousands of tiles fastened to its vulnerable external surfaces. Although the relevant technology might simply be called heat-transfer engineering, the advanced (and still advancing) character of the problems that have to be solved and the consequent need to resort to basic physics and basic fluid mechanics have prompted the practitioners of the field to call it thermophysics. It is the expectation of the editors and the authors of these volumes that the various sections therefore will be of interest to physicists, materials specialists, fluid dynamicists, and spacecraft engineers, as well as to heat-transfer engineers. Volume 77 is devoted to three main topics, Aerothermodynamics, Thermal Protection, and Planetary Entry. Volume 78 is devoted to Radiation Heat Transfer, Conduction Heat Transfer, Heat Pipes, and Thermal Control. In a broad sense, the former volume deals with the external situation between the spacecraft and its environment, whereas the latter volume deals mainly with the thermal processes occurring within the spacecraft that affect its temperature distribution. Both volumes bring forth new information and new theoretical treatments not previously published in book or journal literature.

*Volume 77—444 pp., 6 × 9, illus., \$30.00 Mem., \$45.00 List*

*Volume 78—538 pp., 6 × 9, illus., \$30.00 Mem., \$45.00 List*

TO ORDER WRITE: Publications Dept., AIAA, 1290 Avenue of the Americas, New York, N.Y. 10104